Analysis of Aromatic Delocalization: Individual Molecular Orbital Contributions to Nucleus-Independent Chemical Shifts

Thomas Heine,*,† Paul v. Ragué Schleyer,‡ Clémence Corminboeuf,§ Gotthard Seifert,† Roman Reviakine,|| and Jacques Weber§

Institute of Physical Chemistry and Electrochemistry, TU Dresden, D-01169 Dresden, Germany, Center for Computational Quantum Chemistry (CCQC), Department of Chemistry, University of Georgia, Athens, Georgia 30602-2525, Department of Physical Chemistry, University of Geneva, 30 quai Ernest-Ansermet, CH-1211 Genève 4, Switzerland, and Slovak Academy of Science, Institute of Inorganic Chemistry, SK-84236 Bratislava, Slovakia

Received: April 30, 2003; In Final Form: June 20, 2003

Individual molecular orbital (MO) contributions to the magnetic shielding of atoms as well as to the nucleus-independent chemical shifts (NICS) of aromatic compounds can be computed by the widely used gauge-including atomic orbital (GIAO) method. Detailed analyses of magnetic shielding MO-NICS contributions provide interpretive insights that complement and extend those given by the localized MO ("dissected NICS", LMO-NICS) method. Applications to $(4n + 2)$ π-electron systems, ranging from [n] annulenes to D_{nh} S_3, S_5, and $N_6H_6^{2+}$ rings as well as to D_{2h} cyclobutadiene, show the extent to which their diatropic character results from the σ framework and from the π orbitals. The diatropicity of both these contributions decreases with the number of nodes of the wave function around the ring. The highest-energy orbitals can become paratropic. This is generally the case with the σ orbitals, but is found only for "electron-rich" π systems such as sulfur rings. MO-NICS contributions, which can be interpreted using London−Hückel theory, correlate with inverse ring size.

Introduction

"Aromatic", one of the most used terms in science,[1] describes molecules that benefit energetically from the presence of cyclic or spherical electron delocalization in closed circuits of mobile electrons.[2] The ring currents generated in such molecules by an external magnetic field result in special properties such as "exalted" magnetic susceptibilities[3] and NMR chemical shifts displaced from their normal ranges.[4,5] Such special magnetic influences typically are especially large inside aromatic cyclic or cage molecules. Therefore, Schleyer et al.[6] proposed the NICS method in 1996. NICS is the negative of the magnetic shielding, a well-defined property of electronic systems. At positions reasonably distant from the molecule, this quantity can be accessed experimentally by a chemically inert probe atom at the place where NICS is calculated. Such experiments are well known for fullerenes using ^{3}He nuclei.[7,8] At very low temperatures, it should also be possible to measure physisorbed ^{3}He nuclei above the π system of an aromatic ring, but the distances involved may be too large.

Being based directly on cyclic electron delocalization, which is the essence of aromaticity, NICS is an absolute measure in the sense of not requiring reference standards for its quantification.

However, NICS does not depend purely on the π system but also on other magnetic shielding contributions due to local circulations of electrons in bonds, lone pairs, and atom cores. Because these complicating influences are reduced above ring centers, NICS(1) values (i.e., at points 1 Å away) were recommended as being better measures of π effects than NICS(0) (i.e., in ring centers).[9,10] For planar systems, it is straightforward to separate the NICS contributions of the π system from those of the rest of the molecule. This more refined alternative, "dissected NICS," was introduced in 1997.[10] By employing the decomposition inherent in the IGLO (individual gauge for localized orbitals) method[11] together with Pipek−Mezey localization,[12] the total shieldings are dissected into individual contributions from each localized molecular orbital (LMO). These LMOs generally correspond to individual chemical bonds. For example, the π contributions of planar arenes can be separated from the σ and other contributions. Such sets of related orbitals also can be refined together.[13,14] Statistical analyses have shown $NICS_\pi$ of related series of molecules to be a better measure of aromaticity than total NICS(1) or NICS(0).[15] Other recent studies of magnetic properties include current-density plots,[16] the anisotropy of the current-induced density (ACID),[17] and aromatic ring current shieldings (ARCS).[18,19]

We now discuss contributions of single molecular orbitals to NICS, which can be accessed using the GIAO[20] technique. This new refinement, "MO-NICS analysis", provides complementary insights.[21,22] In view of the large number of chemical shift calculations using GIAO, decomposition into underlined MO contributions will provide many useful results.[5]

Theoretical Basis of the Analysis

Density functional-based calculations of magnetic properties, especially of NMR chemical shifts, provide excellent results for lighter elements.[23−30]

* Corresponding author. E-mail: thomas.heine@chemie.tu-dresden.de.
† TU Dresden.
‡ University of Georgia.
§ University of Geneva.
|| Slovak Academy of Science.

10.1021/jp035163z CCC: $25.00
Published on Web 07/29/2003

TABLE 1: MO NICS Individual Contributions of Low-Energy σ and π Orbitals with Index k[a], NICS, NICS$_\pi$, and LMO-NICS Contributions of σ C−C, S−S, N−N, and C−H Bonds as Well as Lone Pairs (LP) (ppm)

	MO-NICS (GIAO)										LMO-NICS (IGLO)	
	$k=0$		$k=\pm1$		$k=\pm2$		NICS$_{tot}$[c]		NICS$_\pi$		σ framework	
b	σ	π	σ	π	σ	π	IGLO	GIAO	IGLO	GIAO	σ in ring	C−H/LP
$C_3H_3^+$	−25.5	−31.3	−6.9				−21.1	−21.1	−26.0	−31.3	+4.1	−3.1
$C_4H_4^{2+}$	−20.0	−25.3	−3.7				+16.9	+17.2	−20.1	−25.3	+9.3	−0.1
C_4H_4	−17.8	−23.8	−2.6	+25.2			+26.7	+27.3	+4.4	+1.4	+5.8/6.2	−0.3
$C_4H_4^{2-}$	−17.7	−21.0	−5.2	−2.0			−19.9	−15.5	−26.4	−25.0	+2.4	−0.6
$C_5H_5^-$	−12.6	−18.9	−3.8	−3.4			−14.3	−12.3	−22.2	−25.7	+2.2	−0.5
C_6H_6	−8.9	−15.2	−3.6	−5.1			−8.4	−7.2	−20.4	−25.4	+2.5	−0.2
$C_7H_7^+$	−6.1	−11.2	−3.6	−5.5			−6.4	−5.2	−17.5	−22.2	+1.9	−0.2
$C_8H_8^{2+}$	−4.4	−8.4	−3.4	−5.5			−6.9	−6.3	−15.0	−18.9	+1.2	−0.1
$C_8H_8^{2-}$	−4.3	−8.5	−3.1	−4.8	−2.4	−1.8	−14.4	−13.2	−18.8	−21.7	+0.9	−0.2
$C_{10}H_{10}$	−3.0	−5.8	−2.6	−4.4	−2.1	−3.1	−14.0	−13.0	−18.0	−20.8	+0.6	−0.1
S_3	−16.7	−26.3	−1.8	+7.4			−45.6	−45.3	−10.5	−11.5	−9.4	−2.5
S_5	−6.6	−10.3	−3.8	−5.5	−2.3	+5.3	−15.1	−13.6	−10.0	−10.7	−0.2	−1.0
$N_6H_6^{2+}$	−8.5	−13.0	−3.4	−5.9	−2.2	+1.0	−18.7	−17.0	−19.4	−22.8	+10.8	−8.8

[a] Number of nodes around the ring; see eq 1. [b] All geometries have D_{nh} symmetry except C_4H_4. All structures are minima except $C_{10}H_{10}$, S_5, and $N_5H_5^{2+}$. [c] Total NICS given by GIAO and IGLO. The other values constitute only part of the contributions to these totals. For IGLO, the core contributions are not given. For GIAO, many other MO contributions are not given. (See Figure 1.)

In these calculations, except for those with hybrid functionals in some implementations, the coupling of the magnetic field with the potential of the molecule is neglected, and the wave function in the presence of an external magnetic field B is computed as a first-order perturbed quantity.[51]

The theoretical formulation of DFT-NMR calculations, originating with Bieger et al.[31]and Friedrich et al,[32] starts from general quantum electrodynamic (QED) Kohn−Sham-like equations. They made the same assumptions to current-density functional theory[33] as Kohn and Sham did starting from DFT in the Hohenberg−Kohn formulation.[34,35] Within the framework of this theory, the current density $\vec{j}$ is expressed as an orbital-dependent quantity

$$\vec{j}(\vec{r}) = \sum_k n_k \left(\underbrace{\frac{\mathrm{i}}{2}\left(\psi_k \vec{\nabla}\psi_k^* - \psi_k^* \vec{\nabla}\psi_k\right)}_{\text{(I)}} - \underbrace{\frac{1}{c}\vec{A}\psi_k\psi_k^*}_{\text{(II)}} \right) \quad (1)$$

n_k denotes the occupation number, k is the orbital index, A is the vector potential, c is the speed of light, and ψ_k is the molecular orbital. Term (II) of the sum is zero if no magnetic field is applied. In the presence of a magnetic field, this term is called the diamagnetic contribution, and term (I) describes the paramagnetic contribution to the current density. The total current density $\vec{j}$ is a sum over the contributions of all occupied orbitals $\vec{j}_k$. Each contribution $\vec{j}_k$ is directly related to a molecular orbital ψ_k. A gauge transformation applied to this expression would shift contributions from the paramagnetic to the diamagnetic part or vice versa but would not change the orbital contribution of $\vec{j}_k$.

The current density is used to calculate the shielding tensor using Biot−Savart's law. Details are given in Appendix I. Hence, the shielding tensor is calculated for each orbital contribution separately, and the sum of all orbital contributions gives the shielding tensor.

Technical Details of the Computations

Geometries, constrained to D_{nh} symmetry except for D_{2h} C_4H_4, were optimized at the B3LYP/6-31G* level using Gaussian 98.[36] All structures except $C_4H_4^{2+}$, $C_{10}H_{10}$, and S_5 are local minima on the potential energy surface. Chemical shifts are calculated using Kohn−Sham orbitals (PW91/IGLO-III)[11,37] employing the GIAO (gauge-including atomic orbitals)[20] method, here specifically implemented in MAG-ReSpect.[38] Results are compared with the GIAO implementation of ADF,[39] and details of the comparison are given as Supporting Information.

Other computer programs employing the popular GIAO method can be similarly implemented with MO-NICS. Total NICS (or any other chemical shift or shielding value) are separated into contributions from the individual canonical (rather than localized) molecular orbitals. Whereas the total NICS and the total π contributions of a planar arene are, in principle, the same as LMO-NICS,[52] MO-NICS gives the contributions of each π MO separately. This has interpretive advantages in many cases.

Results and Discussion

π System. Table 1 shows that the NICS contributions δ_k ($k = 0, \pm1,...$) from the lowest-energy π MOs ($k = 0$) are the largest. These fall off sharply for the higher degenerate sets of π MOs for the Hückel annulenes with more than one occupied π MO: ($C_4H_4^{2-}$, $C_5H_5^-$, C_6H_6, $C_7H_7^+$, $C_8H_8^{2+}$, $C_8H_8^{2-}$, and $C_{10}H_{10}$). The corresponding MOs and the orbital energies and NICS contributions are shown in Figure 1 for four of those species.

The detailed behavior of the data of Table 1 and Figure 1 can be rationalized by the London−Hückel model, where the ring current susceptibility[40] of a ring π orbital χ_k^π is given by eq 2 (see, for example, ref 41)

$$\chi_k^\pi = \left(\frac{e r_{CC}}{2hc}\right)^2 n^2 \cos\frac{2\pi k}{n} \qquad \text{for } k = 0, \pm1, ... \quad (2)$$

where n is the number of ring atoms and r_{CC} is the C−C bond length. The equation for Hückel orbital energies (eq 3) (see, for example, ref 42) is similar, and each energy, ϵ_k, has the same dependence on the number of nodes $|k|$ as the ring-current susceptibility:

$$\epsilon_k = \alpha - 2\beta\cos\frac{2\pi k}{n} \qquad k = 0, \pm1, \pm2, ... \quad (3)$$

The lowest-energy orbital (with $k = 0$ in eq 1) has the largest value of χ_k^π. These values decrease when going to the higher-energy orbitals ($k = \pm1,...$) and then become negative for $^{|k|}/_n > {}^1/_4$. Davies called this susceptibility "delocalization susceptibility" in order "to avoid misleading analogies suggested by

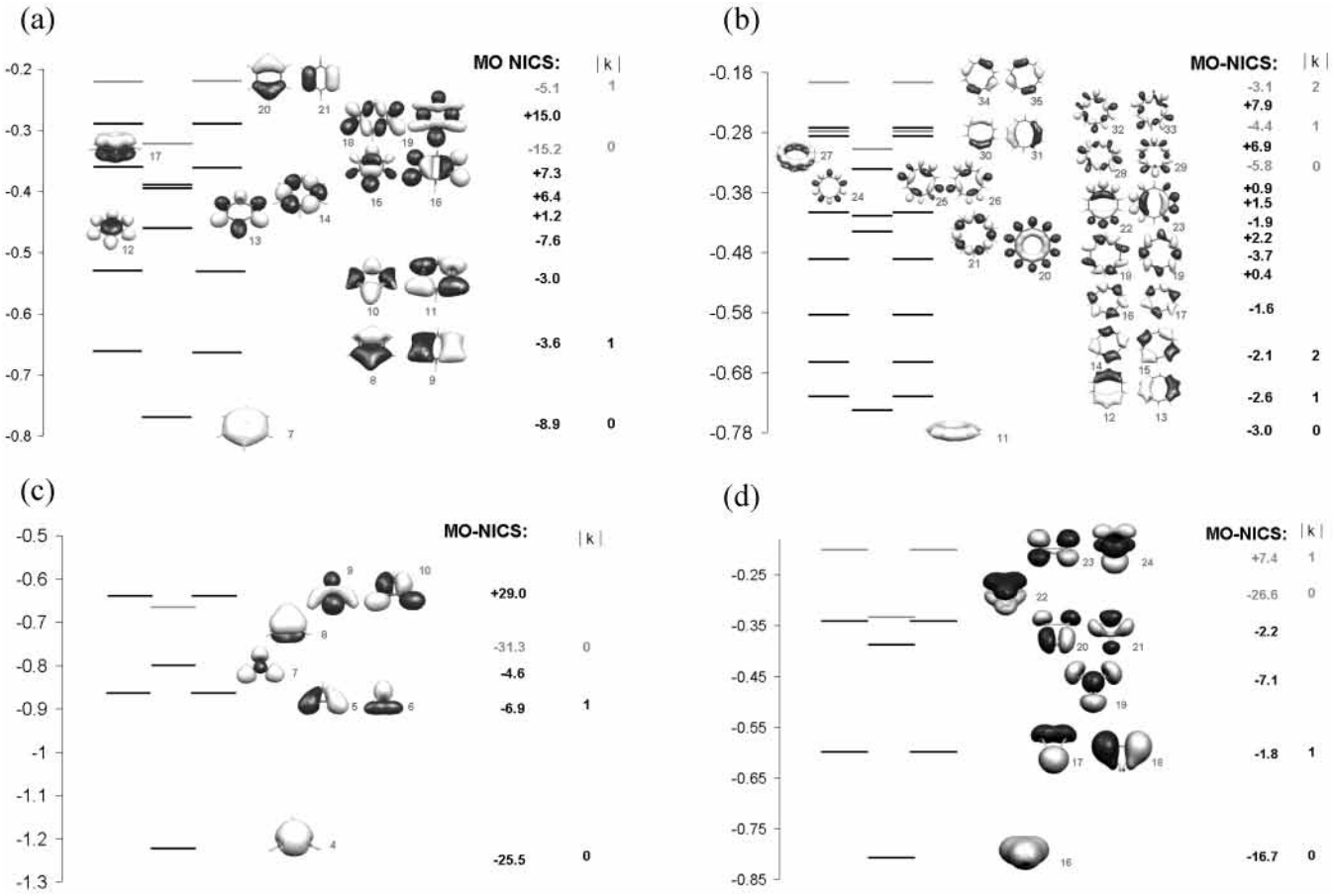

Figure 1. Occupied valence molecular orbitals and their energies in hartrees (in gray for π MOs and in black for σ orbitals). MO-NICS contributions of (a) D_{6h} benzene, (b) D_{10h} $C_{10}H_{10}$, (c) D_{3h} $C_3H_3^+$, and (d) D_{3h} S_3 are given in ppm. Note the large paratropic contributions of the higher-energy σ MOs.

the phrase 'ring current'". The lowest-energy π orbital has the highest degree of delocalization and hence the largest contribution in the energy criterion and for London−Hückel susceptibilities. This is exactly what is found for MO-NICS in Table 1. The contribution of the first π MO always is greater than that of each MO of the first degenerate π set ($k = \pm 1$). The second set of degenerate π MOs in $C_8H_8^{2-}$ and $C_{10}H_{10}$ ($k = \pm 2$) have even smaller contributions.

Both $k = \pm 2$ for $C_8H_8^{2-}$ and $k = \pm 1$ for $C_4H_4^{2-}$ are interesting special cases. Because $^k/_n = {}^1/_4$, the London−Hückel susceptibilities (χ_k^π) are expected to vanish. For simple [n] annulenes, the MO-dependent London−Hückel susceptibility χ_k and the MO contribution of the NICS δ_k at the ring center are related by $\delta_k \approx -\chi_k/n^3$. Indeed, the corresponding MO-NICS contributions are very small (Table 1). If the next higher energy set of degenerate π MOs[53] were occupied (e.g., in $C_3H_3^{3-}$ and $C_5H_5^{5-}$), then even their MO contributions should be deshielding (paratropic).

Although such π occupancies are unrealistic for hydrocarbon polyanions because of the excessive Coulomb repulsion, neutral, isoelectronic analogues (e.g., the D_{nh} sulfur clusters with "extra π electrons", S_n ($n = 3$ and 5)) confirm these expectations (Table 1). The $k = \pm 1$ π orbitals of D_{3h} S_3 have a paratropic MO-NICS of +7.4 ppm each. Each of the $k = \pm 2$ π-orbital contributions of D_{5h} S_5 is +5.3 ppm. These findings demonstrate that π orbitals of cyclic compounds with ($4n + 2$) π electrons are not always diatropic. Even for D_{6h} $N_6H_6^{2+}$, a 10-π-electron molecule isoelectronic to $C_6H_6^{4-}$, the $k = \pm 2$ π MOs are slightly paratropic (+1 ppm). Although the quantum chemical results differ quantitatively from the approximate London−Hückel predictions for the large $|k|$ values discussed here, the expected trend is followed.

Aromatic [n] annulenes are well known to have diatropic total NICS, although the IGLO LMO dissection reveals that some of the individual contributions (especially those of the σ CC bonds) are paratropic.[9,10,14,43] The same is true for MO-NICS, where the contributions from MOs with no nodes or only a few nodes around the ring are diatropic but those from orbitals with more nodes are paratropic. Whereas the trends are the same for both σ and π MOs, more σ than π orbitals are occupied. Consequently, the contributions from π MOs always are diatropic (except in molecules with extra π electrons, e.g., S_3, S_5, and $N_6H_6^{2+}$; see Table 1). This behavior can be rationalized by simple Hückel theory. The MO energies (ϵ_k from eq 2 for cyclic π systems) have the same dependency on the node index k as the MO susceptibilities (eq 1). The MO susceptibilities and therefore the MO-NICS are diatropic for bonding MOs, whereas the orbitals giving paratropic contributions have antibonding Hückel energies (although, as in S_3 and S_5, they can still be electron binding in full quantum chemistry computations). However, their energies are lower in nonplanar geometries where orbital mixing can take place. Hence, such extra electron ($4n + 2$) π-electron systems (i.e., Hückel aromatic ($4n + 2$) π-electron molecules with $|k| > {}^n/_4$ occupied orbitals are seldom planar because better nonplanar geometries exist, e.g., C_s symmetry for S_5 or D_{3d} for $N_6H_6^{2+}$). Exceptions arise only when planarity is inevitable, as in cyclic S_3, or is forced by constraints of the σ framework.

NICS of antiaromatic cyclobutadiene (D_{2h}) is strongly paratropic (Table 1); $NICS_\pi$ very small.[43] This can be understood

using MO-NICS: In C_4H_4, two π orbitals are occupied—the low-energy orbital and a $k = 1$ orbital. This orbital has a strong paratropic contribution because it has a node through the whole molecule and cancels the highly diatropic π-orbital effect.

Nonaromatic planar $(CH_2)_n$ rings have been studied with LMO-NICS and MO-NICS by Moran et al. The contribution of the π system was found to be negligible, but Walsh and σ contributions are important.[21]

Our results seem to contradict those of Steiner, Fowler, and co-workers,[44,45] who show that only the frontier orbitals of [n] annulenes exhibit a ring-current density when an external magnetic field is applied and that the lower-energy orbitals do not contribute to the ring current at all. What we calculate here are not the same quantities: Steiner and Fowler discuss ring-current densities parallel to the molecular plane arising from a perpendicular magnetic field. In contrast, NICS is the trace of the shielding tensor, which takes into account the magnetic field applied in all three space directions (see eq 4 in Appendix I). Indeed, the MO contributions of the frontier orbitals are dominated by the *zz* component of the shielding tensor, which arises from a current density in the *xy* plane, and the $k = 0$ orbitals have considerable contributions from all components of the shielding tensor. The results of MO-NICS and current-density plots will be compared in more detail in a forthcoming publication.

***σ*-Framework Contributions to MO-NICS and Ring Size Dependence.** Figure 1 shows that the framework σ molecular orbitals of annulenes typically have the same symmetry patterns as the π orbitals (when viewed from the *z* axis normal to the ring). In particular, note the corresponding shapes of the π and low-energy σ framework orbitals; the only major differences are the π-orbital nodes in the *xy* plane.

Like the combinations of the singly occupied p_z AOs in Hückel's π theory, the lowest-energy σ valence orbitals are composed almost exclusively of C 2s orbitals, one per carbon. Consequently, MO-NICS for both sets of MOs are similar: both are always diatropic. This is exemplified by the equivalence of σ orbitals 7 (A_{1g}), 8, and 9 (E_{1u}) of benzene and the corresponding π orbitals, 17 (A_{2u}) and the degenerate HOMO, 20 and 21 (E_{1g}) (Figure 1). The energy differences between these σ and π MOs as well as their MO-NICS contributions also are similar. Hence, the total NICS of a ring can depend as strongly on the low-energy σ-framework MOs as on the π MOs.[9,10,46]

The remaining higher-energy benzene framework MOs (MO 10 and higher) are 2s, $2p_x$, and $2p_y$ carbon hybrid orbitals, involved with CH as well as with CC bonding. With one exception, there is a clear trend from less diatropic to ever more paratropic contributions with increasing numbers of nodes. The highest occupied σ MOs (18 and 19) are very paratropic. The exception, the highly symmetrical diatropic MO 12 ($2A1_g$), has six overlapping lobes in the center. With "σ-aromatic" character and no nodes around the ring, 12 is the "in-plane" counterpart of 17, the lowest π MO ($3A1_g$).[47] The MO-NICS of the lowest-energy orbitals of the σ framework and of the π system are related quantitatively for the whole series of rings from $C_3H_3^+$ to $C_{10}H_{10}$, but ring-size effects are substantial.[48] For the regular Hückel [n] annulenes, δ_k should be proportional to $^1/_n$ (see eq 1 and the relation between χ_k and δ_k). Indeed, as shown by Figure 3, the MO-NICS contributions by the lowest σ and the lowest π MOs correlate reciprocally with the ring size.

Conclusions

In summary, the individual MOs of both σ framework and π sets in cyclic aromatic molecules can either be diatropic or paratropic depending on the number of nodes around the ring. As the MOs increase in energy (and the nodal complexity increases), the diatropicity first decreases and then the paratropicity increases (Figure 1). Because the rings have a greater number of σ than π electrons, higher-energy σ orbitals with many nodes are occupied. These are paratropic (Figure 1).

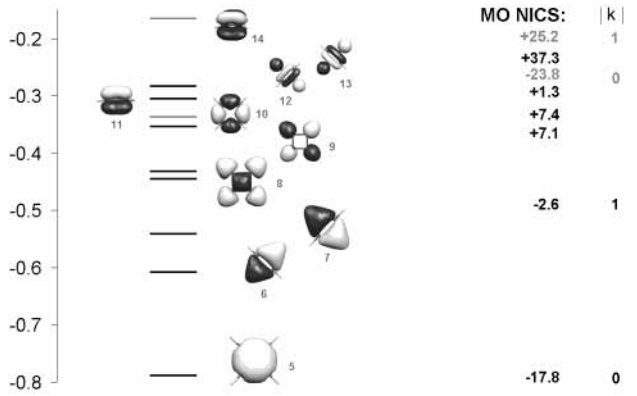

Figure 2. Occupied valence molecular orbitals and their energies in hartrees (in gray for π MOs and in black for σ orbitals). MO-NICS contributions of D_{2h} C_4H_4.

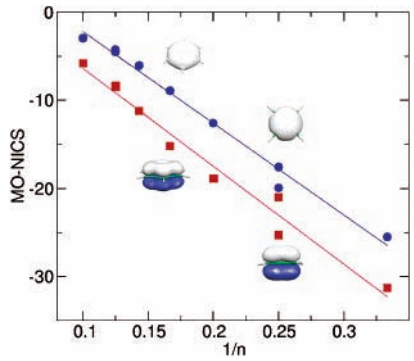

Figure 3. MO-NICS of the lowest-energy ($k = 0$) σ orbitals (red) and π orbitals (blue) correlate with the inverse number of ring atoms, $^1/_n$ for [n] annulenes $C_{10}H_{10}$ to $C_3H_3^+$ from left to right.

In contrast, the higher-energy paratropic π orbitals usually are not occupied in the typical aromatic molecules because they are Hückel antibonding. Consequently, $NICS_\pi$ is diatropic for $(4n + 2)$ [n] annulenes. However, the top set of π MOs are occupied in the extra-electron $(4n + 2)$ e planar S_3, S_5, and $N_6H_6^{2+}$ species; their paratropic contributions (Figure 1 and Table 1) decrease the $NICS_\pi$ to values substantially lower than those of the $C_3H_3^+$, $C_5H_5^-$, and C_6H_6 counterparts.

The contributions of both the σ and π $k = 0$ MOs, and hence the total NICS diatropicity, fall off with ring size. However, this effect is counterbalanced to some extent by the greater number of electrons of the larger rings. $C_8H_8^{2+}$ and $C_8H_8^{2-}$ are essentially the same size, but the latter is more aromatic because it has four more π electrons. Whereas the total π contributions change only modestly in going to the larger rings (Table 1), the falloff per ring carbon is appreciable.[5]

The MO-NICS and the dissected LMO-NICS[10] methods are nicely complementary. Whereas the total NICS are, in principle, the same, their decompositions are different. Both give the total π NICS, but MO-NICS differentiates among the individual occupied π MOs. LMO-NICS gives the individual σ CC and CH as well as the localized π contributions: the CH and CC π effects are diatropic, but the CC σ contributions are paratropic.[9] MO-NICS does not differentiate the framework effects but provides a detailed analysis of the contributions of each

canonical molecular orbital. MO-NICS applies well to 3D and "spherical" species, where 2D ring-current models and LMO-NICS are not adequately informative. Studies of such systems are currently in progress.

Of course, both the MO and LMO decomposition methods can be used generally, for example, for the analysis of the origins of NMR chemical shifts of the constituent atoms in molecules.[11]

Acknowledgment. We thank Alexei Arbouznikov and the MAG-ReSpect developers[38] for code distribution and Dr. Serguei Patchkovskii for valuable discussions. We acknowledge financial support from Graduiertenkolleg "Heterocyclen" of TU Dresden, the Swiss National Science Foundation, the University of Georgia, and National Science Foundation (U.S.) grant CHE-0209857.

Appendix

I. MO Analysis of the Magnetic Shielding Tensor. *The Shielding Tensor as a Property of the Current Density*. An external magnetic field $\vec{B}_0$ induces a magnetic field at the nuclei of a sample (solid, ensemble of molecules). This field, acting on a nucleus at position $\vec{R}$, can be written in the following form:

$$\vec{B}_{\mathrm{loc}} = \frac{1}{c}\int \frac{\vec{j}(\vec{r}) \times (\vec{r} - \vec{R})}{(\vec{r} - \vec{R})^3}\,\mathrm{d}^3r + \frac{8\pi}{3}\langle \vec{M}_S(\vec{R})\rangle$$

The first term (Biot-Savart's law) comes from the orbital current density $\vec{j}$, and the second term is caused by the magnetization density at the nucleus. The induced field $\vec{B}_{\mathrm{loc}}$ defines the shielding tensor of nucleus *k*:

$$\sigma_{uv}^{(k)} = \frac{\partial(\vec{B}_{\mathrm{loc}})_u^{(k)}}{\partial(\vec{B})_v}$$

In current-density functional theory (CDFT),[33] the current density in the presence of an applied magnetic field has the form

$$\vec{j}(\vec{r}) = \sum_k n_k \frac{\mathrm{i}}{2}(\psi_k \vec{\nabla}\psi_k^* - \psi_k^* \vec{\nabla}\psi_k) - \frac{1}{c}\vec{A}\psi_k\psi_k^*$$

and can be written in a Taylor expansion with respect to the applied magnetic field $\vec{B}$:

$$\vec{j}(\vec{B},\vec{r}) = \vec{j}_0(\vec{r}) + \vec{B}\frac{\partial \vec{j}(\vec{B},\vec{r})}{\partial \vec{B}} + \ldots.$$

The current density in a free, closed-shell molecule without an applied external magnetic field is zero, and $\vec{j}_0$ vanishes. The derivative in the first member of the Taylor expansion is a tensor and henceforth will be given as

$$\overleftrightarrow{j}_1 = \frac{\partial \vec{j}(\vec{B},\vec{r})}{\partial \vec{B}}$$

In the same way, the molecular orbitals, orbital energies, and Kohn−Sham matrices can be expanded in Taylor series. The orbitals can be written as

$$\psi_k(\vec{B}) = \psi_{k0} + \vec{B}\cdot\frac{\partial \psi_k}{\partial \vec{B}} + \ldots = \psi_{k0} + \vec{B}\cdot\vec{\psi}_{k1} + \ldots.$$

Because the shielding tensor is linear in $\vec{B}$, only the linear terms of these series need to be considered. This leads to a sum over all occupied states *k*:

$$\vec{B}\cdot\overleftrightarrow{j}_1(\vec{r}) = \sum_k n_k \vec{B}\cdot(\vec{\psi}_{k1}\otimes\vec{\nabla}\psi_{k0}^* - \psi_{k0}\vec{\nabla}\otimes\vec{\psi}_{k1}^*) - \frac{1}{2c}(\vec{B}\times\vec{r})\psi_{k0}\psi_{k0}^* \quad (4)$$

n_k denotes the occupation number of orbital *k*. The final expression for the shielding tensor is

$$\overleftrightarrow{\sigma} = -\frac{\mu_0}{c}\frac{\partial}{\partial \vec{B}}\int \frac{(\vec{B}\cdot\overleftrightarrow{j}_1)\times\vec{R}}{(\vec{r} - \vec{R})^3}\,\mathrm{d}^3r \quad (5)$$

Orbital Contributions to the Current Density in Current-Density Functional Theory. Current-density functionals are practically unavailable at present. Therefore, Bieger, Friedrich, and co-workers's proposal of an "uncoupled" treatment for DFT using perturbation theory[31,32] is the theoretical basis of all current applications of DFT-NMR calculations. In this treatment, the coupling between the molecular orbitals and the first-order perturbed wave function is usually neglected.

Because density functional theory is a one-particle theory, the contribution of each single molecular orbital can be accessed in eq 4. Hence, it is possible to decompose the shielding tensor into single molecular orbital contributions in a straightforward way. This is even possible for coupled CDFT if a current-density exchange correlation potential would be available.

II. Influence of the Gauge Problem. The shielding tensor must be independent of the gauge origin. However, the number of basis functions is always limited in actual computations. Hence, the choice of gauge is a practical problem for the calculation of magnetic properties.[49,50] Several methods allow calculations with moderate basis sets at reasonable accuracy. The gauge-including (in original terminology, gauge-invariant) atomic orbital (GIAO) method is the most widely applied: the gauge origin is included explicitly in each basis function. GIAO has also been chosen for our analysis because it is the most convenient way to obtain the orbital contributions to the shielding tensor.

For comparison, we computed orbital contributions to the shielding tensor with ADF[39] for two molecules, $C_3H_3^+$ and C_6H_6 (Tables 2 and 3). The NMR-EPR implementation of the ADF computer code by G. Schreckenbach provides an excellent analysis tool for the quite demanding GIAO expressions. Following the implementation of Schreckenbach and Ziegler, the paramagnetic part has three contributions (given in the same order as in ref 26): the first arises directly from the GIAO gauge transformation, the second describes occupied−occupied contributions, also induced by the gauge transformation, and the last one is the conventional paramagnetic term expressed in occupied−unoccupied matrix elements. The occupied−occupied matrix elements are completely symmetric and hence contribute in equal part to both orbitals.

Supporting Information Available: Decomposition of diatropic and paratropic contributions of valence orbitals of $C_3H_3^+$ and C_6H_6. This material is available free of charge via the Internet at http://pubs.acs.org.

References and Notes

(1) Krygowski, T. M.; Cyranski, M. K. *Chem. Rev.* **2001**, *101*, 1385.
(2) Schleyer, P. v. R. *Chem. Rev.* **2001**, *101*, 1115.

(3) Dauben, H. J., Jr.; Wilson, J. D.; Laity, J. L. *J. Am. Chem. Soc.* **1968**, *90*, 811.
(4) Günther, H. *NMR Spectroscopy: Basic Principles, Concepts, and Applications in Chemistry*, 2nd ed.; Wiley: Chichester, U.K., 1995; p 581.
(5) Wannere, C. W.; Schleyer, P. v. R. *Org. Lett.* **2003**, *5*, 605.
(6) Schleyer, P. v. R.; Maerker, C.; Dransfeld, A.; Jiao, H.; Eikema Hommes, N. J. R. *J. Am. Chem. Soc.* **1996**, *118*, 6317.
(7) Bühl, M.; Patchkovskii, S.; Thiel, W. *Chem. Phys. Lett.* **1997**, *275*, 14.
(8) Saunders, M.; Jimenez-Vazquez, H. A.; Cross, R. J.; Billups, W. E.; Gesenberg, C.; Gonzalez, A.; Luo, W.; Haddon, R. C.; Diederich, F.; Herrmann, A. *J. Am. Chem. Soc.* **1995**, *117*, 9305.
(9) Schleyer, P. v. R.; Manoharan, M.; Wang, Z., X.; Kiran, B.; Jiao, H.; Puchta, R.; Eikema Hommes, N. J. *Org. Lett.* **2001**, *3*, 2465.
(10) Schleyer, P. v. R.; Jiao, H.; Eikema Hommes, N. J. R.; Malkin, V. G.; Malkina, O. *J. Am. Chem. Soc.* **1997**, *119*, 12669.
(11) Kutzelnigg, W. *Isr. J. Chem.* **1980**, *19*, 193.
(12) Pipek, J.; Mezey, P. G. *J. Chem. Phys.* **1989**, *90*, 4916.
(13) Gregor, T.; Mauri, F.; Car, R. *J. Chem. Phys.* **1999**, *111*, 1815.
(14) Corminboeuf, C.; Heine, T.; Weber, J. *Phys. Chem. Chem. Phys.* **2003**, *5*, 246.
(15) Cyranski, M. K.; Krygowski, T. M.; Katritzky, A. R.; Schleyer, P. v. R. *J. Org. Chem.* **2002**, *67*, 1333.
(16) Fowler, P. W.; Steiner, E.; Zanasi, R.; Cadioli, B. *Mol. Phys.* **1999**, *96*, 1099.
(17) Herges, R.; Geuenich, D. *J. Phys. Chem. A* **2001**, *105*, 3214.
(18) Juselius, J.; Straka, M.; Sundholm, D. *J. Phys. Chem. A* **2001**, *105*, 9939.
(19) Juselius, J.; Sundholm, D. *Phys. Chem. Chem. Phys.* **1999**, *1*, 3429.
(20) Ditchfield, R. *Mol. Phys.* **1974**, *27*, 789.
(21) Moran, D.; Manoharan, M.; Heine, T.; Schleyer, P. v. R. *Org. Lett.* **2003**, *5*, 23.
(22) Corminboeuf, C.; Heine, T.; Weber, J. *Org. Lett.* **2003**, *5*, 1127.
(23) Malkin, V. G.; Malkina, O. L.; Casida, M. E.; Salahub, D. R. *J. Am. Chem. Soc.* **1994**, *116*, 5898.
(24) Malkin, V. G.; Malkina, O. L.; Salahub, D. R. *Chem. Phys. Lett.* **1993**, *204*, 80.
(25) Malkin, V. G.; Malkina, O. L.; Salahub, D. R. *Chem. Phys. Lett.* **1993**, *204*, 87.
(26) Schreckenbach, G.; Ziegler, T. *J. Phys. Chem.* **1995**, *99*, 606.
(27) Cheeseman, J. R.; Trucks, G. W.; Keith, T. A.; Frisch, M. J. *J. Chem. Phys.* **1996**, *104*, 5497.
(28) Schreckenbach, G.; Ziegler, T. *Theor. Chem. Acc.* **1998**, *99*, 71.
(29) Bühl, M.; Kaupp, M.; Malkina, O. L.; Malkin, V. G. *J. Comput. Chem.* **1999**, *20*, 91.
(30) Wang, B.; Fleischer, U.; Hinton, J. F.; Pulay, P. *J. Comput. Chem.* **2001**, *22*, 1887.
(31) Bieger, W.; Seifert, G.; Eschrig, H.; Grossmann, G. *Chem. Phys. Lett.* **1985**, *115*, 275.
(32) Friedrich, K.; Seifert, G.; Grossmann, G. *Z. Phys. D: At., Mol. Clusters* **1990**, *17*, 45.
(33) Rajagopal, A. K.; Callaway, J. *Phys. Rev. B: Solid State* **1973**, *7*, 1912.
(34) Kohn, W.; Sham, L. J. *Phys. Rev. A* **1965**, *140*, 1133.
(35) Hohenberg, P.; Kohn, W. *Phys. Rev. B* **1964**, *136*, 864.
(36) Frisch, M. J.; Trucks, G. W.; Schlegel, H. B.; Scuseria, G. E.; Robb, M. A.; Cheeseman, J. R.; Zakrzewski, V. G.; Montgomery, J. A., Jr.; Stratmann, R. E.; Burant, J. C.; Dapprich, S.; Millam, J. M.; Daniels, A. D.; Kudin, K. N.; Strain, M. C.; Farkas, O.; Tomasi, J.; Barone, V.; Cossi, M.; Cammi, R.; Mennucci, B.; Pomelli, C.; Adamo, C.; Clifford, S.; Ochterski, J.; Petersson, G. A.; Ayala, P. Y.; Cui, Q.; Morokuma, K.; Malick, D. K.; Rabuck, A. D.; Raghavachari, K.; Foresman, J. B.; Cioslowski, J.; Ortiz, J. V.; Stefanov, B. B.; Liu, G.; Liashenko, A.; Piskorz, P.; Komaromi, I.; Gomperts, R.; Martin, R. L.; Fox, D. J.; Keith, T.; Al-Laham, M. A.; Peng, C. Y.; Nanayakkara, A.; Gonzalez, C.; Challacombe, M.; Gill, P. M. W.; Johnson, B. G.; Chen, W.; Wong, M. W.; Andres, J. L.; Head-Gordon, M.; Replogle, E. S.; Pople, J. A. *Gaussian 98*, revision A.8; Gaussian, Inc.: Pittsburgh, PA, 1998.
(37) Perdew, ; Wang, Y. *Electronic Structure of Solids '91*; Academie Verlag: Berlin, 1991; p 11.
(38) Malkin, V. G.; Malkina, O.; Reviakine, R.; Schimmelpfennig, B.; Arbrouznikov, A.; Kaupp, M. *MAG-ReSpect* 1.0; 2001.
(39) Te Velde, G.; Bickelhaupt, F. M.; Baerends, E. J.; Fonseca Guerra, C.; Van Gisbergen, S. J. A.; Snijders, J. G.; Ziegler, T. *J. Comput. Chem.* **2001**, *22*, 931.
(40) London, F. *J. Phys. Radium* **1937**, *8*, 397.
(41) Davies, D. W. *The Theory of the Electric and Magnetic Properties of Molecules*; Wiley: London, 1967.
(42) Heilbronner, E.; Bock, H. *The HMO Model and its Application*; Wiley: London, 1976.
(43) Schleyer, P. v. R.; Kiran, B.; Simion, D. V.; Sorensen, T. S. *J. Am. Chem. Soc.* **2000**, *122*, 510.
(44) Steiner, E.; Fowler, P. W. *J. Phys. Chem. A* **2001**, *105*, 9553.
(45) Steiner, E.; Fowler, P. W. *Chem. Commun.* **2001**, 2220.
(46) Fowler, P. W.; Havenith, R. W. A.; Steiner, E. *Chem. Phys. Lett.* **2001**, *342*, 85.
(47) Schleyer, P. v. R.; Jiao, H.; Glukhovtsev, M. N.; Chandrasekhar, J.; Kraka, E. *J. Am. Chem. Soc.* **1994**, *116*, 10129.
(48) Wannere, C. W.; Schleyer, P. v. R. *Org. Lett.* **2003**, *5*, 865.
(49) Hegstrom, R. A.; Lipscomb, W. N. *J. Chem. Phys.* **1968**, *48*, 809.
(50) Lipscomb, W. N. *Adv. Magn. Reson.* **1966**, *2*, 137.
(51) The shielding tensor is a second-order property; however, it is linear with respect to $\vec{B}$. See also Appendix I.
(52) The IGLO and GIAO data in Table 1 vary somewhat quantitatively because of inherent differences in the two methods.
(53) $k = \pm 2$ for $C_5H_5^{5-}$, $C_6H_6^{4-}$, and $C_7H_7^{3-}$, and $k = \pm 3$ for $C_8H_8^{6-}$ and $C_{10}H_{10}^{4-}$.